Article

Coastal Aquifer Salinization in Semi-Arid Regions: The Case of Grombalia (Tunisia)

Siwar Kammoun [1],*[ID], **Rim Trabelsi** [1], **Viviana Re** [1,2,3][ID] **and Kamel Zouari** [1]

1   Laboratory of Radio-Analyses and Environment, National School of Engineers of Sfax, BP1173, Sfax 3038, Tunisia; trabelsi.rim01@gmail.com (R.T.); viviana.re@unipi.it (V.R.); kamel.zouari@enis.tn (K.Z.)
2   Department of Molecular Sciences and Nanosystems, Ca' Foscari University of Venice, Via Torino 155, 30170 Venezia-Mestre, Italy
3   Earth Sciences Department, University of Pisa, Via Santa Maria, 53, 56126 Pisa, Italy
*   Correspondence: siwarkammoun@gmail.com

Abstract: Groundwater resources are facing increasing pressure especially in semi-arid regions where they often represent the main freshwater resource to sustain human needs. Several aquifers in the Mediterranean basin suffer from salinization and quality degradation. This study provides an assessment of Grombalia coastal aquifer (Tunisia) based on multidisciplinary approach that combines chemical and isotopic (δ^2H, δ^{18}O, ^{3}H, ^{14}C and δ^{13}C) methods to characterize the relation between groundwater quality variation and aquifer recharge. The results indicate that total dissolved solids exceed 1000 mg/L in the most of samples excepting the recharge area. In addition to water–rock interaction, evaporation and nitrate pollution contributing to groundwater mineralization, the reverse cation exchange process constitute an important mechanism controlling groundwater mineralization with enhancing risk of saltwater intrusion. Environmental isotope tracers reveal that groundwater is evolving within an open system to close system. A significant component of recent water that is recharging Grombalia aquifer system is confirmed by applying correction models based on the δ^{13}C values and ^{14}C activities and tritium contents. However, this recharge, which is mainly associated to the return flow of irrigation water, contributes to the groundwater salinization, especially for the shallow aquifer.

Keywords: groundwater; mineralization; water–rock interactions; cation exchange process; isotopes; aquifer recharge

1. Introduction

In arid and semi-arid regions worldwide, local populations mainly rely on groundwater resources to sustain domestic, industrial and agricultural needs [1–3]. Despite their vital role, however, aquifers are exposed to multiple pressures resulting in over-exploitation, quality degradation and salinization [1,4,5].

This is the case of the Cap Bon peninsula (northeastern Tunisia), which is one of the most developed regions in the country in terms of agriculture, industry and tourism. These water-intensive activities are exerting pressure on local resources, resulting in several issues that need to be addressed to ensure the wellbeing of the local population and the long-term environmental protection of the region [3,6–9]. In addition, as in the case of many arid and semi-arid regions, the over-exploitation of already limited water resources, coupled with increasing water demand and the irregularity of the rainfall regime due to climate changes is likely to exacerbate the competition on water use among different sectors and may become a driver for social instability [10,11]. In fact, in this region and especially in the rural areas, the water supply network is not available for all the inhabitants, and, hence, most of them depend on groundwater to satisfy their basic needs [11].

Understanding the processes and factors controlling the temporal dynamic of the chemical groundwater composition is therefore essential to guide decision-makers towards a rational and more sustainable management of these resources.

To this end, this work presents the results of an integrated assessment performed in the Cap Bon peninsula, and in particular in the Grombalia aquifer, the most important agricultural area in this region. During the past decade, the intensive exploitation of the Grombalia groundwater resources has largely influenced the water quality, exposing the system to saline intrusion due to the increasing groundwater abstraction near to the coast [12]. In addition, domestic and industrial activities are contributing to both groundwater exploitation and aquifer recharge associated to wastewater disposal. This anthropogenic recharge can therefore have a severe influence on the groundwater quality that needs to be assessed. Even though other studies [7,10,13–16] have focused on this aquifer, the complexity to determine all the multiple processes contributing to aquifer salinization and the different recharge processes still need to be fully understood.

To shed some light on these processes, this work presents an integrated chemical and isotopic assessment of the whole aquifer system targeting aquifer recharge modes and their influence on groundwater quality and salinization. Overall, the aim of the present investigation is to trace groundwater origin and its residence time. To achieve these goals, a combined use of geochemical and isotopic ($\delta^{18}O$, δ^2H, ^3H, ^{14}C and $\delta^{13}C$) tracers was adopted to study the main processes controlling groundwater mineralization and its relation with the aquifer recharge.

The findings of this study will be very useful to improve management strategies to protect scarce groundwater resources in the region, as well as to deepen the knowledge on the status of coastal aquifers in the Mediterranean basin.

2. Site Description

The Grombalia coastal aquifer is located in the Cap Bon peninsula (latitudes 36°29′00″– 36°42′00″ N and longitudes 10°27′00″–10°47′00″ E), and it extends over an area of approximately 719 km². It is bordered by Bouchoucha Mountain (Mt.) and Halloufa Mt. to the west, the anticline of Abderrahman Mt. and Takelsa syncline to the east, the plain of Hammamet to the south and the Gulf of Tunis to the north (Figure 1). The region is characterized by a semi-arid Mediterranean climate, influenced by humid air masses coming from the Mediterranean Sea, with the irregularity of the rainfall in time and in space. The average annual rainfall is about 506 mm/year. Climatic conditions of the Cap Bon peninsula favor the development of agriculture in this region which provides around 16% of the national agricultural production [6]. Thus, the plain of Grombalia is one of the most important agricultural regions in Tunisia.

The Grombalia region represents a graben geology structure oriented northwest–southeast and filled by Quaternary deposits composed of a multi-layered aquifer system. The phreatic unconfined aquifer is composed of the Quaternary continental deposits, mainly with sand, sandstones and clayey sand, tapped by many wells at depths varying from 15 to 40 m limited by clay layer substratum of about 15 m thickness [16]. The confined deep aquifer is housed in Miocene sandstone (about 35 m average thickness) tapped by many boreholes at depths ranging 60–160 m. The different aquifer levels communicate with each other due to the discontinuity of marl layers [17].

Grombalia aquifers are defined as over-exploited state. In fact, the water withdrawal of the shallow aquifer increased from 85 Mm³ in 2005 to 104 Mm³ in 2014 (extracted by 8814 wells) exceeding the available resources estimated at 51 Mm³/year. For the deep aquifer, the exploitation was estimated at 21.6 Mm³ in 2014 (extracted by 578 boreholes), while the renewable resources are estimated at 9.5 Mm³/year [18]. As a response, the Medjerda-Cap Bon canal was set up by the local authorities, in 1984, to ensure the transfer of surface water collected in several dams built on the Medjerda basin, characterized by good quality with a total dissolved solids (TDS) less than 1000 mg/L, from the northwest of Tunisia to

the Grombalia region. These water resources have been mainly used for basic needs as irrigation and drinking water and also for the artificial recharge of water in some sites.
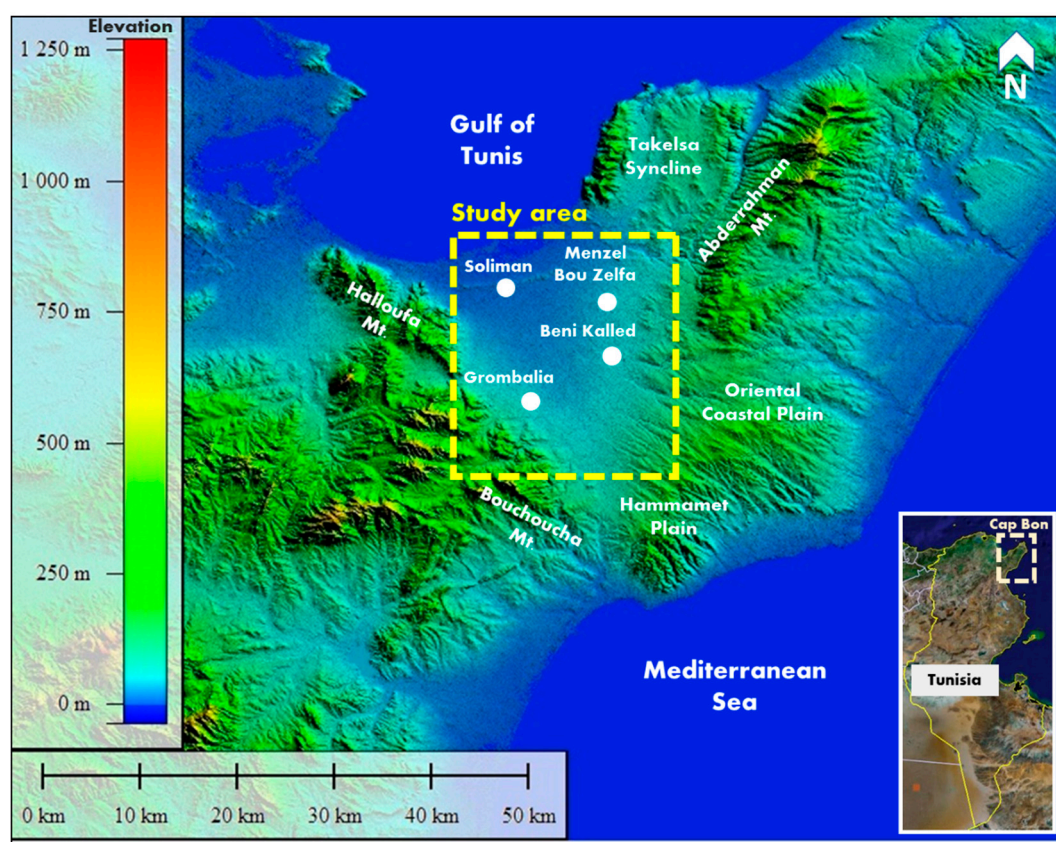

Figure 1. Location and elevation maps of the study area, Grombalia region, (northeast of Tunisia) produced from SRTM (Shuttle Radar Topography Mission) map.

In addition, artificial recharge of water was adopted in 1972 through sand infiltration basins and direct water injection in some wells. However, the artificial recharge which is carried out from the infiltration basins was stopped in 2011.

The recharge of the aquifer is mainly occurred in the east part of the basin, precisely in the pediment of Abderrahman mountain, and converges to the north of Grombalia towards the Gulf of Tunis (discharge area) [7,11,14,16], with SE–NW groundwater flow direction. The piezometric levels of shallow and deep aquifers converge from the south (the foothills of Abderrahman Mt.) to the north of the plain (Gulf of Tunis). Piezometric levels range from 60 to 10 m in the shallow aquifer and from 140 to 20 m for the deep one.

3. Materials and Methods

To assess the geochemical evolution of salinity in the Grombalia aquifer, an hydrochemical and isotopic characterization was performed on 53 samples collected in March 2014 (27 groundwater samples in the deep aquifer and 26 in shallow) [11] and 14 samples from the deep aquifer collected in March 2017. To better assess the temporal variations of the aquifer system, chemical and isotopic results were also compared with those of previous investigation carried out in 2005 [13,17].

For the 2014 and 2017 samples, physico-chemical parameters (Temperature (T°), electrical conductivity (EC) and potential hydrogen (pH)) were measured on site during sample collection using a WTW 340i multi-meter. Chemical and isotopic analyses were performed at the Laboratory of Radio-Analyses and Environment (LRAE) at the National School of Engineers of Sfax (Tunisia). Major elements (HCO_3^-, Cl^-, SO_4^{2-}, NO_3^-, Na^+, Mg^{2+}, Ca^{2+} and K^+) were analyzed by high-performance liquid chromatography (HPLC-

Waters) with less than $\pm5\%$ value of the ionic balance. The partial pressure of carbon dioxide (pCO_2) was calculated using Diagrammes software (Ver. 6.7) [19].

Water stable isotope analyses ($\delta^{18}O$ and δ^2H) were performed using laser absorption spectrometry, LGR DLT 100, [20]. Isotope results are reported in delta value expressed in ‰ VSMOW (Vienna Standard Mean Oceanic Water) with the measurements uncertainly of ±0.1‰ for $\delta^{18}O$ and 1‰ for δ^2H. Samples were analyzed for tritium contents using electrolytic enrichment and liquid scintillation counter [21] and expressed in tritium units (TU) with a precision of measurement equal to ±0.3 TU. Carbon−14 analyses were performed on all the samples collected in March 2017. Samples were precipitated as $BaCO_3$ and measured through benzene synthesis and liquid scintillation spectrometry [22]. The results are expressed as percent of modern carbon (pmc) with an analytical uncertainty of 1 pmc. The $\delta^{13}C$ values ($^{13}C/^{12}C$ ratios) are expressed relative to V-PDB (Vienna-Pee Dee Belemnite) standard with an uncertainty equal to ±0.3‰. The spatial distribution maps of the TDS values were performed based on geostatistical approach using the kriging technique for data modelling using the software package of Arc GIS (Ver. 10.3).

4. Results and Discussion

4.1. Mineralization Origin

4.1.1. Salinity Evolution: Application of Geostatistical Mapping Tools

A fundamental step in any groundwater quality assessment, is to determine the geochemical processes controlling natural mineralization and the anthropogenic sources affecting water composition. It is also necessary to study the behavior of dissolved ions in water and to examine the spatiotemporal evolution of salinity (hereafter expresses as TDS, as the sum of major elements concentrations expressed in mg/L).

Many natural factors contribute to groundwater mineralization: (i) the source of recharge water and its chemical composition; (ii) the lithological and hydrological characteristics of the aquifer matrix; (iii) groundwater residence time; and (iv) the chemical processes occurring within the aquifer.

To evaluate the groundwater mineralization, TDS distribution maps for samples collected in 2014 [11] were elaborated.

For the shallow aquifer, TDS values vary between 715–6357 mg/L (Table S1) and increase from the south to the Gulf of Tunis, coherently with the southeast–northwest groundwater flow directions. On the other hand, in deep aquifer, TDS range from 727.2 to 10,177.4 mg/L, and the highest values are found in the center of the basin between Beni Kalled and Grombalia cities (e.g., Samples No. 107, 108 and 118 in Figure 2). As a first approximation based on this evidence, the study region can be subdivided into two different zones according to the recommended TDS value for drinking use (1000 mg/L [23]) (Figure 2).

The first zone is characterized by low salinity (TDS < 1000 mg/L), in the south and south-eastern part of the basin at the foot of the border reliefs (Abderrahman Mt.) and the oriental coastal plain. The lowest TDS values characterize the upstream portion of the area and may be linked to direct infiltration of freshwater from the recharge areas.

The second zone corresponds to samples with high salinity (TDS > 1000 mg/L), located in the central and northwestern part of the study area. The increase of salinity for the shallow aquifer, observed near the coast (Gulf of Tunis), can be explained by a supply of saline water from the Sebkha (salt deposits) and/or the sea. High TDS values observed for the deep aquifer in the central part can be associated to the presence of evaporates deposits.

Therefore, the large variation of TDS values reflects the interference of several processes that affect the chemical composition of the shallow and deep groundwater in Grombalia basin.
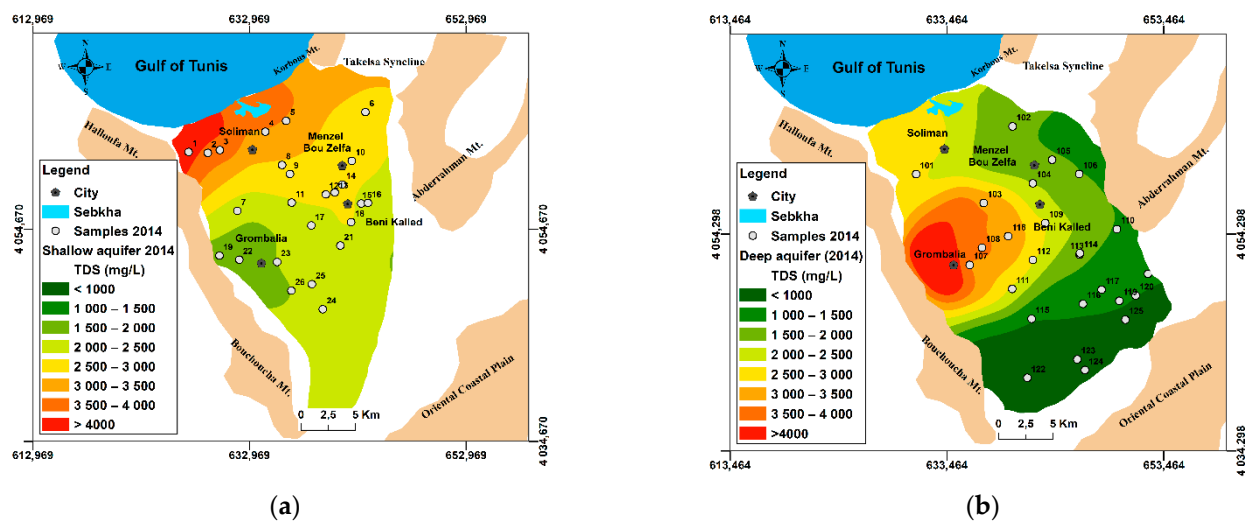
(a)

(b)

Figure 2. Distribution map of TDS values for samples collected in 2014 using the ordinary kriging method with: (**a**) shallow aquifer; and (**b**) deep aquifer.

For a long time, the Grombalia aquifer has been considered as an important groundwater resources providing a good water quality used for several needs as drinking water and agricultural development. However, in the two past decades, the overexploitation of the shallow aquifer has caused water quality degradation. The main mechanism contributing to aquifer salinization, as pointed out in previous works [10,11,13,15–17,24,25], is the dissolution of evaporate minerals such as halite (NaCl), gypsum ($CaSO_4$ $2H_2O$) and anhydrite ($CaSO_4$). This process was highlighted by the strong correlation between Na^+ versus Cl^- and between Ca^{2+} versus SO_4^{2-}. On the other hand, the poor correlation observed between calcium and bicarbonate in the previous studies cited above, indicates the precipitation of carbonate minerals existing in the sedimentary deposits. This process was highlighted by over-saturation state (saturation index > 1) for most of samples with respect to calcite, aragonite ($CaCO_3$) and dolomite ($CaMg(CO_3)_2$). Thus, Ca^{2+} excess and Na^+ deficiency characterizing some samples suggest the existence of other mechanisms of mineralization that significantly affect groundwater quality, such as the ion exchange process.

According to the position of the points on the Ca+Mg versus HCO_3+SO_4 diagram [9] (Figure 3), three major groups of groundwater have been identified. The first group (G1) includes samples falling along the 1:1 line corresponding to gypsum, calcite and dolomite dissolution showing the dissolution of these minerals [26], but in the present study area only dissolution of gypsum is retained regarding to saturation index values [11]. The second group (G2) is represented by just a few samples from the deep aquifer showing a slight increase in the concentration of SO_4+HCO_3 over Ca+Mg, suggesting the dissolution of sulfate minerals. Finally, the third group (G3) comprises by samples with dominance of Ca+Mg over HCO_3+SO_4 mainly for shallow aquifer that can be a result of reverse cation exchange process [27], by which the sodium ions are fixed on the surface of clay minerals against the release of calcium.

The ion exchange process is confirmed if studying the relation $[Na^+ + K^+ - Cl^-]$ versus $[(Ca^{2+} + Mg^{2+}) - (HCO_3^- + SO_4^{2-})]$, as reported in [28] for both shallow and deep aquifers (Figure 4). This figure shows that the majority of samples fall on a straight line with a slope equal to −1 [26], confirming that sodium, calcium and magnesium minerals significantly participate in the ion exchange reactions. In addition, in this figure, three groups of water are determined, as discussed in the previous paragraph. A first group composed by samples close to the origin point indicates dissolution phenomenon and the absence of exchange reactions [29]. The second group represented by few samples of deep aquifer falls in the direct ion exchange trend by which sodium minerals are fixed on the surface of clay minerals against the release of calcium. The third group gathers the majority of samples characterized by reverse ion exchange process with release of Ca

and adsorption of Na. In addition, the calculation of Ca + Mg/HCO$_3$ ratio is helpful to understand the origin of water. In the case of fresh recharge of the aquifer with meteoric nature of groundwater, this ratio should be less than 1 [9].
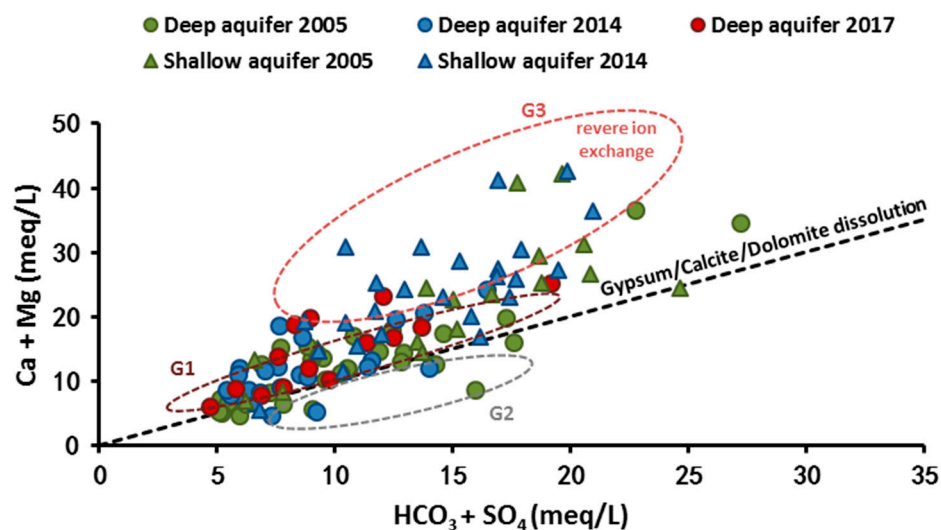

Figure 3. Plot of Ca + Mg versus HCO$_3$ + SO$_4$.

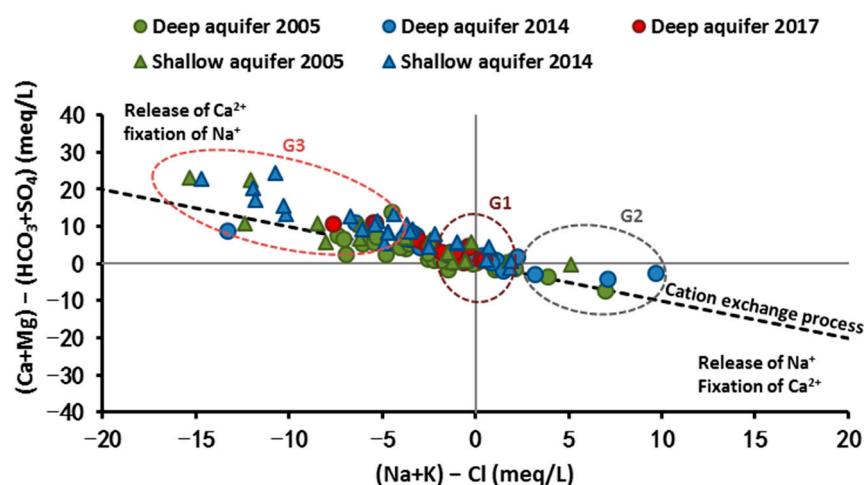**Figure 4.** Relationship of (Na + K) − Cl versus (Ca + Mg) − (HCO$_3$ + SO$_4$).

Overall, all samples have a very high Ca+Mg/HCO$_3$ ratio [9] (varying between 0.7 and 27.1) with only three samples with ratio less than 1, thus showing that fresh groundwater recharge in the studied region is probably limited [9], and/or there are some processes that significantly affect its quality by increasing calcium concentration. The excessive amount of calcium may be attributed to geogenic factors (i.e., ion exchange process, so-called natural enrichment). The various processes governing the overall water chemistry of the studied aquifer were explored further by applying the hydrochemical facies evolution diagram, as described in the following paragraph.

4.1.2. Salinity Origin: Use of Hydrochemical Facies Evolution Diagram

Hydrochemical facies evolution diagram (HFE-D) [30] has been successfully used to assess the origin of groundwater salinization and to identify the different trends of freshening or salinization in coastal aquifer (e.g., [5,31–34]). Therefore, to understand the state of Grombalia coastal aquifer and to discriminate between the different phases

(salinization or freshening) that takes place over time, thus contributing to groundwater mineralization, hydrochemical facies evolution diagram (HFE-D) was studied.

Four major facies are identified in this diagram [30]: Ca–HCO$_3$ for freshwater (FW), Na–Cl for seawater (SW), Ca–Cl representing saline water with reverse cation exchange and Na–HCO$_3$ for salinized water with direct cation exchange. The freshening and salinization phases are separated by the conservative mixing line (CML). Each phase is divided into sub-stages: f1, f2, f3, f4 and FW for freshening phase and i1, i2, i3, i4 and SW for salinization phase. The distribution of major ions percentages in the HFE-square diagram (Figure 5) shows that samples situated above the CML are representative of the freshening state, while samples below and to the right of CML indicate the trend of salinization phase.

The HFE square diagram (Figure 5) represents the distribution of the major mineral percentages for 2005 [13,18], 2014 [11] and 2017 groundwater samples. The 2005 data are used as a term of comparison to better highlight possible temporal variations and the evolution of the system after 7 and 12 years.

For the 2005 campaign, samples from shallow aquifer are characterized by the dominance of the i2 + i3 + i4 (76%) sub-stages relative to the f1 +f2 (23%) sub-stages (Figure 5a). Nine years later, in 2014, about 65% of samples belongs to i4 + i3 + i2 sub-stages and 35% to f1 + f2 + f3 (Figure 5b), suggesting the trend of the shallow aquifer towards the equilibrium state mainly due to the significant recharge of the aquifer.

For the deep aquifer, samples representing the 2005 (Figure 5c) campaign are grouped in the i1 + i2 + i3 (43%) and f1 + f2 + f3 + f4 (57%) sub-stages. For the 2014 campaign (Figure 5d), samples are characterized by the dominance of the i1 + i2 + i3 (68%) relative to the f1 + f3 + f4 (32%) sub-stages and samples of 2017 are grouped as 50% for i1 + i2 + i3 and 50% for f1 + f2 + f3 + f4 sub-stages (Figure 5e). Nevertheless, the dispersion of some samples in the f1 and f2 sub-stages, corresponding to freshening phase, suggest that the Grombalia aquifer tries to reach the equilibrium state. For the shallow aquifer, most samples fall within the Mix Ca−Cl, Mix Na–Cl and Ca–Cl water types and some samples belong to Na–Cl, Na–HCO$_3$ and Ca–HCO$_3$ facies. For the deep aquifer, samples can be grouped into four groundwater facies based on their position on the HFE plot. These groups are classified in descending order as follows: Mixed Ca–Cl > Mixed Na–Cl > Ca–Cl > Na–Cl > Na–HCO$_3$ > Ca–HCO$_3$.

The major water type in Grombalia aquifer consists of mixed Ca−Mg−Cl, representing the evolved hydrochemical facies, in which the initial meteoric signature has been changed due to many factors such as water–rock interactions and ion exchange process. Only few groundwater samples (from 2014 and 2017 campaigns) belong to the Na–Cl type, indicating the evaporation process that contribute to groundwater chemical composition.

The Ca–Cl water type mainly occurs due to the cation exchange process where sodium is removed from solution and calcium is released [5,9,35]. Typically, this type of water is characterized by very high TDS values owing to the high concentration of calcium and chloride minerals [9] which could be related to seawater intrusion. It is demonstrated in [35] that, in the case of marine water intrusion, when saline water reaches the aquifer that was previously occupied by fresh water type, a chemical reaction happens generating the release of Ca^{2+} and the adsorption of Na$^+$ in a reverse base exchange phenomenon (Na$^+$ + Ca– [clay] → Ca^{2+} + [clay] –Na). In this case, the water evolves from a Ca–HCO$_3$ meteoric type to Na−Cl facies, via an intermediate Ca–Cl water type. Therefore, for Grombalia aquifer, as the major groups of water are Mixed Ca–Cl and Mixed Na–Cl, defined as intermediate water type to sea water intrusion, the risk of marine intrusion exists.
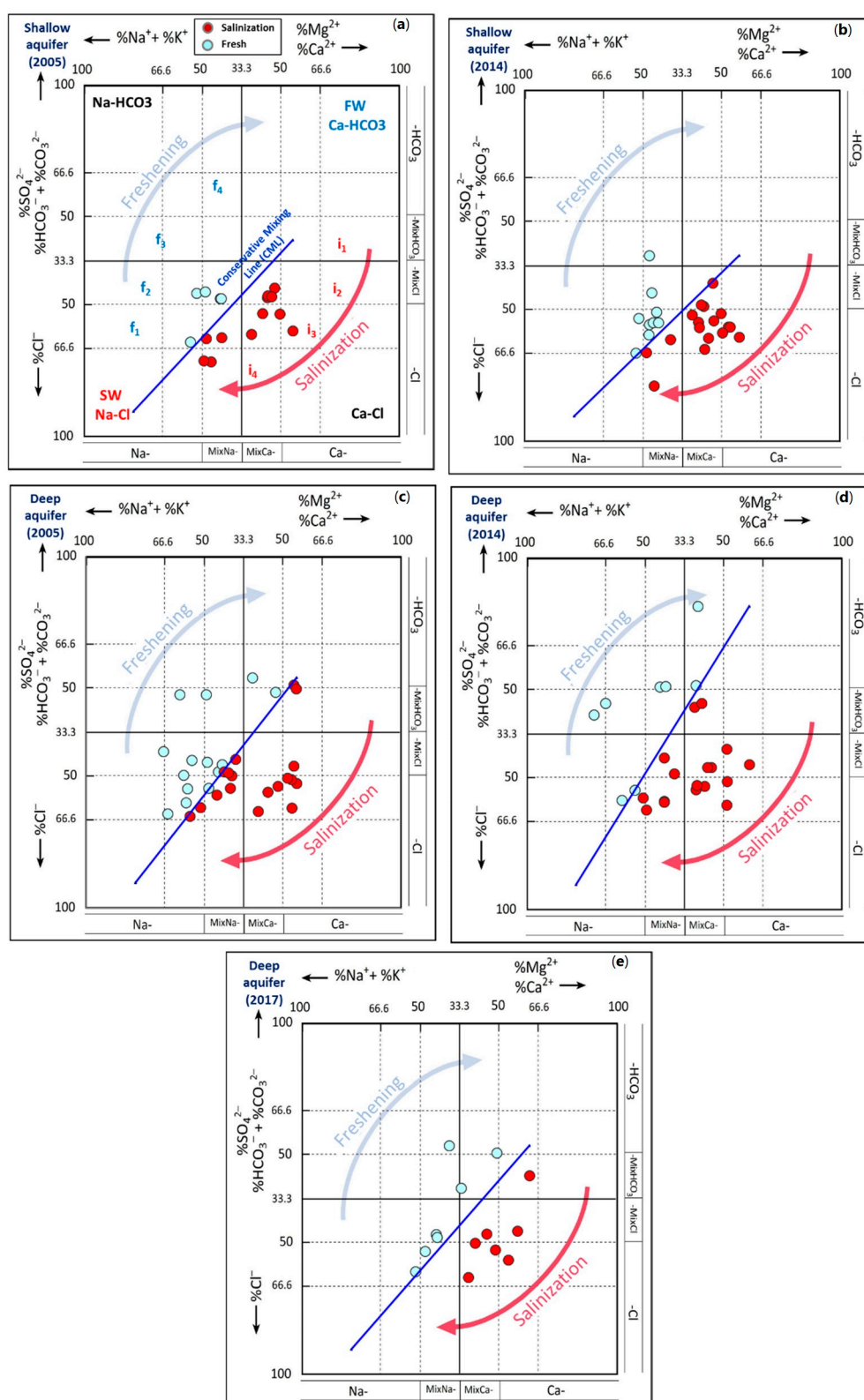
Figure 5. Representation of groundwater samples on the Hydrochemical Facies Evolution Diagram (HFE-D; modified after [30]) with: (**a**) shallow aquifer 2005; (**b**) shallow aquifer 2014; (**c**) deep aquifer 2005; (**d**) deep aquifer 2014; and (**e**) deep aquifer 2017. Red circles correspond to samples with trend to salinization and Blue circles correspond to samples with trend to freshening.

Overall, the return flow of irrigation water and the over-exploitation of groundwater resources have been identified as sources of salinization in the center of the plain highlighted by the direct ion exchange process. The very high groundwater salinity observed near the coast (Gulf of Tunis) could be explained by the presence of a marine water intrusion.

This hypothesis is based on the very high calcium and chloride concentrations, in addition to the presence of reverse ion exchange reactions and the hydrochemical facies variation. Seawater intrusion hypothesis should be confirmed by the piezometric map. In the case of seawater intrusion, piezometric levels should be below sea level. Until now, the seawater intrusion phenomenon cannot be confirmed or excluded, because of the lack of data and the absence of deep piezometers covering the whole area especially on the north of the plain near the coast. This topic thus requires further investigation.

4.2. Recharge Processes and Water Quality Variation

4.2.1. Water Stable Isotopes ($\delta^{18}O$ and δ^2H)

Isotope investigation is of paramount importance in groundwater studies. It provides fundamental information that facilitates the understanding of the functioning of the aquifer system. Therefore, it permits to identify the origin and the age of water, the recharge rate and the residence time of water within an aquifer. In addition, this approach is useful to highlight certain mineralization processes, in particular the mixture between different types of water [36].

For the isotopic characterization of Grombalia groundwater, two reference lines were used: the global meteoric water line (GMWL) following Equation (1) [37],

$$\delta^2H = 8.17\ \delta^{18}O + 10.35 \tag{1}$$

and the local meteoric water line of Tunis-Carthage (LMWL) according to Equation (2) [38]:

$$\delta^2H = 8\ \delta^{18}O + 12.4 \tag{2}$$

The isotopic composition in the study area ranges between −6.1‰ and −3.1‰ VS-MOW for $\delta^{18}O$ and between −37.1‰ and −20.8‰ VSMOW for δ^2H (Table S1), although the samples show a high variability in their distribution (Figure 6). In fact, two groups of water can be distinguished.
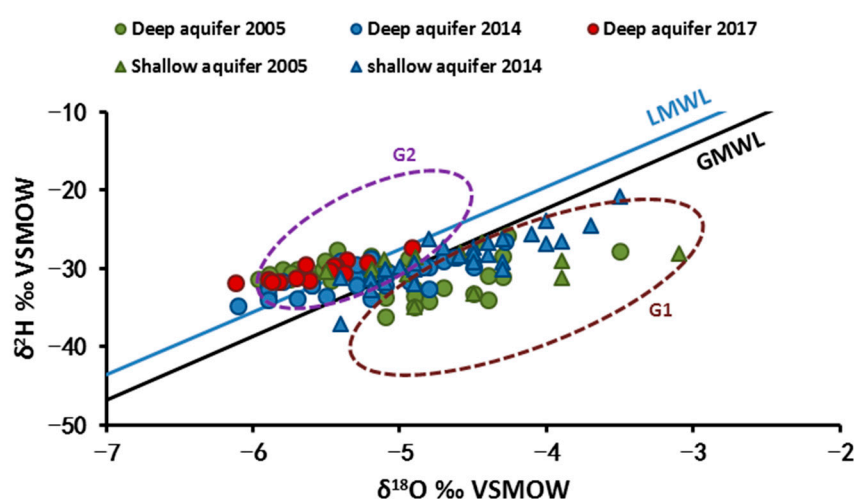

Figure 6. Diagram $\delta^{18}O-\delta^2H$ of Grombalia groundwater. The black line corresponds to the Global Meteoric Water Line (GMWL) and the blue line corresponds to the Local Meteoric Water Line of Tunis-Carthage (LMWL).

The first group is characterized by the most enriched samples, generally from the shallow aquifer, plot below the two reference lines (GMWL and LMWL). These samples

are located between Menzel Bou Zelfa and Beni Kalled agricultural regions, which are principally dominated by citrus cultivation (Figure 7a,b). This trend might indicate the recharge of the aquifer by evaporated meteoric water and/or the return flow of evaporated irrigation water. Furthermore, few groundwater samples (Nos. 4 and 5), the most enriched in δ^{18}O and δ^2H, suggest an eventual mixture with saline water from the Sebkha.
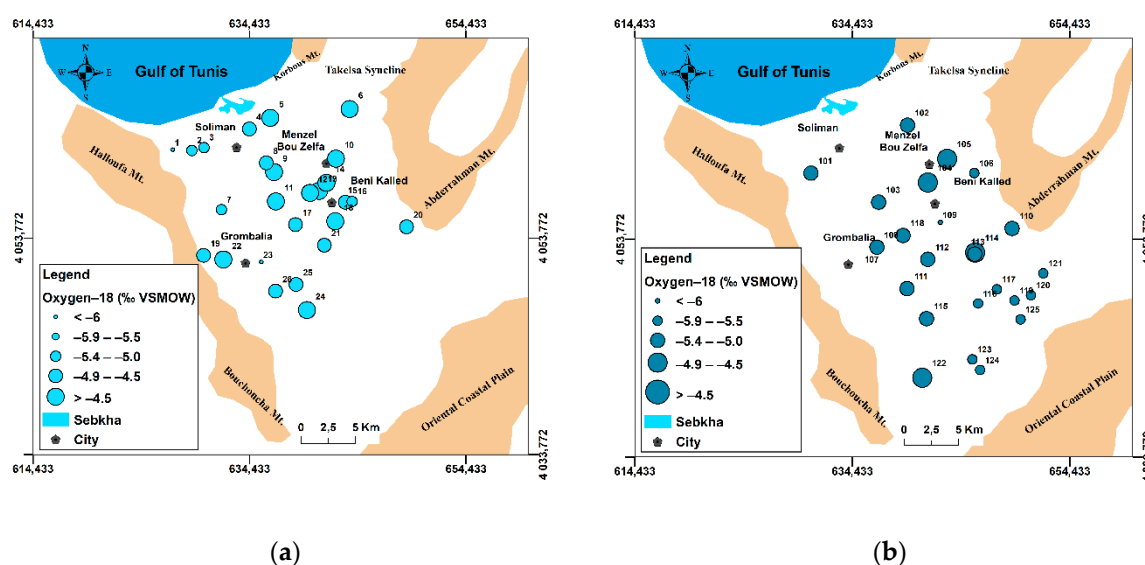

(**a**)   (**b**)

Figure 7. Distribution map of oxygen−18 (‰ VSMOW) for samples collected in 2014 with: (**a**) shallow aquifer; and (**b**) deep aquifer.

The second group represents the majority of samples, situated close to the LMWL and GMWL. The mean isotopic compositions of this group, about −4.3‰ and −24.8‰ VSMOW for δ^{18}O and δ^2H, is similar to those of current local precipitation, as measured at the meteorological station of Tunis-Carthage [39]. This signature, characteristic of the most aquifers of Cap Bon region [8], indicates the presence of recent recharge by rapid infiltration of meteoric water that has escaped the phenomenon of evaporation.

The analysis of the relationship between δ^{18}O and chloride concentrations provides several information on the mechanisms responsible for aquifer mineralization. The δ^{18}O/Cl$^-$ diagram shows that samples enriched in δ^{18}O present high chloride concentrations (more than 700 mg/L) reducing the infiltration of evaporated brackish to saline water (Figure 8).

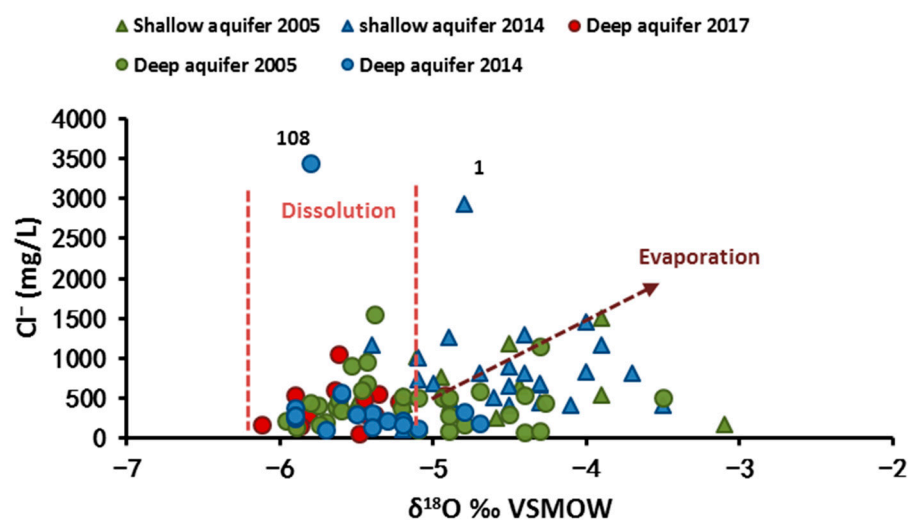**Figure 8.** Diagram δ^{18}O/ Cl$^-$ of Grombalia groundwater.

However, the majority of the deep aquifer samples show low levels of oxygen-18 and high levels of chloride. The absence of any correlation in this aquifer demonstrates the interference of several process responsible of groundwater mineralization. Therefore, for the deep aquifer, the dissolution mechanism outweighs the phenomenon of evaporation in groundwater. This dissolution can be contemporaneous or subsequent to the infiltration in the unsaturated zone or within the aquifer itself. The highest value of TDS (10,177 mg/L) observed in deep groundwater Sample No. 108 (at depth 86 m) is mostly related to the abundance of sulfate contents [24] close to Grombalia city. In fact, this sample presents the highest concentration of chloride (3436 mg/L), sulfate (3105 mg/L), sodium (1888 mg/L) and magnesium (557 mg/L).

4.2.2. Tritium Isotope

Tritium (^{3}H), the radioactive isotope of hydrogen, has been proven to be an excellent tracer to estimate water age [40]. In particular, its short half-life of approximately 12.32 $\pm$ 0.02 years [41] makes it useful to identify recent groundwater recharge (<50 years) [42]. Its presence in groundwater provides evidence for active recharge. In fact, in 1952, a peak concentration of tritium was recorded in precipitation, produced by thermonuclear testing. Since 1962, tritium concentrations have been gradually declined as a result of radioactive decay and the cessation of atmospheric nuclear tests.

The tritium contents in the Grombalia groundwater samples vary between 0 and 3.6 $\pm$ 0.1 TU for the deep aquifer and between 0.6 and 5.6 TU for the shallow aquifer. As shown on the ^{3}H/TDS diagram (Figure 9a), more than 70% of water samples indicate significant values of tritium greater than 1 TU. The high ^{3}H contents confirm the modern infiltration of recent waters (post 1952) in the Grombalia basin, particularly in the shallow aquifer. Only a few samples show low tritium values (i.e., less than 1 TU). This indicates either the ancient origin of the waters or the existence of a mixing phenomenon between recent and old waters. This hypothesis is discussed further using the radioactive isotope carbon-14 activities.
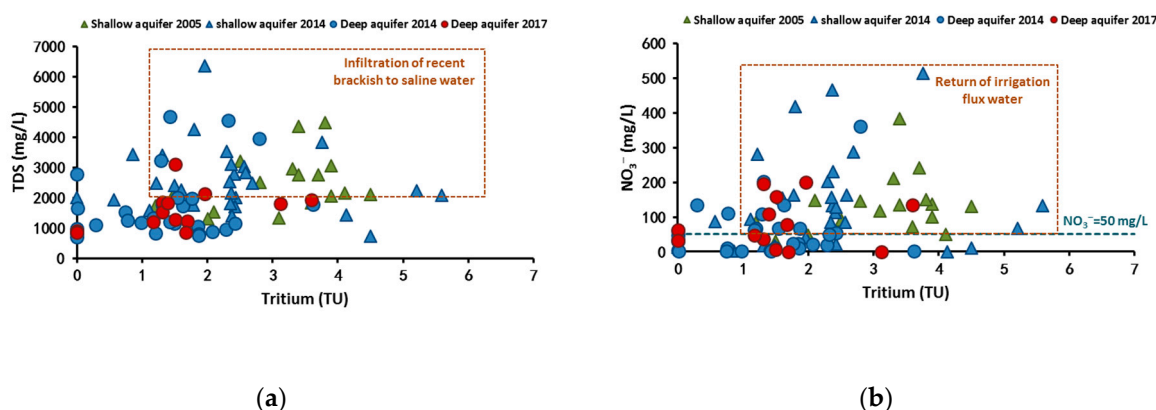

Figure 9. Variation of tritium contents in groundwater samples according to: (**a**) total dissolved solids (TDS) values; and (**b**) NO_3^-.

The variation of tritium contents in groundwater samples according to NO_3^- concentrations indicate that samples with high nitrate contents greater than 50 mg/L (the statutory limit for drinking water) [23] also contain significant tritium values (^{3}H > 1 UT) (Figure 9b), especially for the shallow aquifer. This could be explained by the recent origin of nitrate contamination proving the contribution of return flow of irrigation water, enriched in nitrate fertilizers, to aquifer recharge.

However, samples of the deep aquifer are scattered and do not show significant correlation between tritium and nitrates. In fact, being the deep aquifer generally characterized by low nitrate concentrations (NO_3 <50 mg/L), the tritium values greater than 1 UT can be indicative of the absence of nitrate pollution, dilution phenomena or the dominance of

denitrification process. For the 2014 sampling campaign, approximately 53% of the shallow aquifer samples (depth varying 12–35 m), and only one sample from the deep aquifer (No. 102, at depth 70 m), are characterized by high TDS values (>2000 mg/L), high nitrate contents (>50 mg/L) and significant tritium value (>1 TU). These samples are located in the northern part of the plain, close to the agricultural and industrial city of Soliman (Nos. 3–5) and between Beni Kallel and Menzel Bou Zelfa regions where the agriculture activities are dominants (Nos. 6, 9, 12–17 and 21). Sample No. 25 situated close to Grombalia city and was collected from a large irrigated perimeter owned by the government for the production of citrus fruits. This confirms that the impact of return flow irrigation on groundwater quality is more significant in the shallow aquifer. Consequently, the infiltration of the superficial irrigation's water enriched with nitrate fertilizers has an important role in the aquifer recharge and groundwater salinization especially for shallow aquifer.

4.2.3. Carbon-13 Isotope

Environmental isotope tracers are particularly useful for identifying the origin of salinity and the recharge processes of the aquifer. Previous studies show that most aquifers of the Cap Bon peninsula are characterized by a significant recharge of recent waters [8,10,13] occurring mainly during the Holocene [8]. The measure of carbon-13 stable isotope is therefore essential to understand the nature of the system and to correct groundwater residence time estimated by carbon-14.

The $\delta^{13}C$ values of the total dissolved inorganic carbon (TDIC) of samples collected in 2005 range from $-15.53‰$ to $-10‰$ for shallow aquifer and from $-14.39‰$ to $-8.87‰$ V-PDB for the deep aquifer [11]. For the deep groundwater samples collected in 2017, $\delta^{13}C$ values vary between $-13.14‰$ and $-11.12‰$. This wide range of values indicates the presence of several sources of dissolved carbon in groundwater system.

The partial pressure of carbon dioxide (pCO_2) has an important role in the water chemistry. It reflects the geochemical process and influences the reactions between the CO_2 coming from the atmosphere, biological activity and carbonate rocks dissolution (carbonates and bicarbonates) [43].

The calculated values of log (pCO_2) are negative for all samples, varying between -2.86 and -0.52. This shows that these waters have gained the carbon dioxide resulting from the organic matter degradation in the soil and from some plants [44].

The plot of $\delta^{13}C$ relative to log (pCO_2) (Figure 10) indicates that samples with high pCO_2 values and depleted in $\delta^{13}C$ were recorded in the upstream part (south and southeast) of the basin, especially in the foothills of the border reliefs (Abderrahman Mt.). This reflects an interaction with the CO_2 of the soil, giving an open system and recent recharge of water that crossed the entire unsaturated zone. Low values of pCO_2 and enriched $\delta^{13}C$, characterizing the coastal region, result mainly from the strong interaction of water with the aquifer's matrix [45] under closed system.
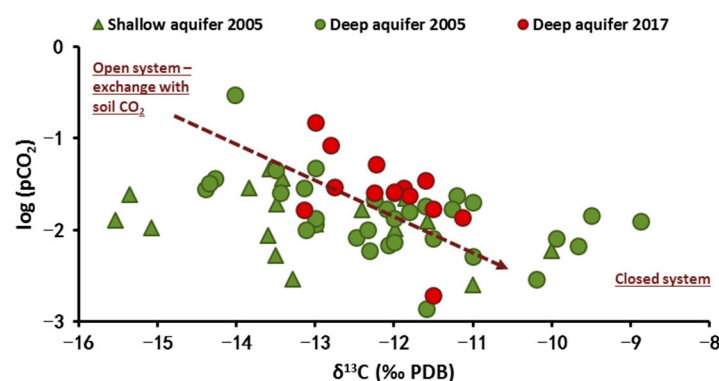

Figure 10. Plot of groundwater $\delta^{13}C_{TDIC}$ signatures versus log (pCO_2).

The relationship between $\delta^{13}C$ signatures according to Mg^{2+}/Ca^{2+} (Figure 11) confirms the role of the dissolution of carbonates in water mineralization. The presence of CO_2, under an open system favors the dissolution of carbonate minerals existing in the aquifer matrix. This reaction will lead to a progressive enrichment in carbon-13.
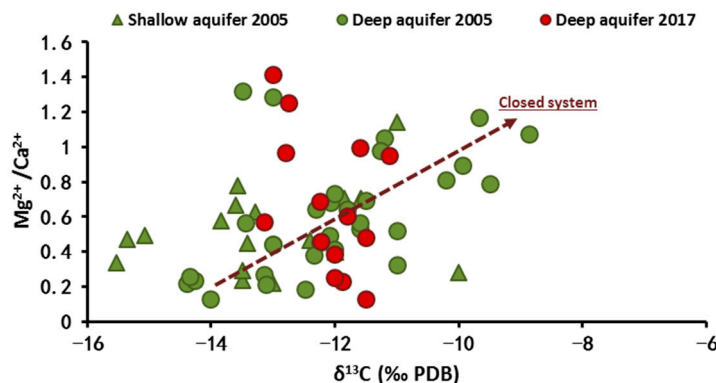

Figure 11. Plot of groundwater $\delta^{13}C_{TDIC}$ signatures versus Mg^{2+}/Ca^{2+}.

The simultaneous increase of Mg^{2+}/Ca^{2+} with $\delta^{13}C$ values characterizing most of the samples from the deep aquifer suggests the incongruent dissolution caring out at saturation state towards the calcium [46]. In fact, the increase in $\delta^{13}C$ of TDIC with the increase of the of Mg^{2+}/Ca^{2+} ratio highlight an evolution towards closed system.

Nitrate contamination represents a serious problem in the Grombalia region, as studied in [25], proving the multiple origins of nitrate pollution associated to both agricultural and domestic activities. In Grombalia region, the structured interviews to local farmers, administered during the sampling campaigns and in situ measurements, provided useful information about the nature of used fertilizers [25]. It revealed that farmers mainly use manure in combination with synthetic fertilizers: manure (16%); three-component synthetic fertilizers (NPK) (10%); manure and NPK (37%); manure, DAP and NPK (32%); and DAP and NPK (5%). The isotopic investigation performed by Re et al. [25] also highlighted the dual origin of nitrate pollution: urban/domestic and agricultural origins.

The plot of groundwater $\delta^{13}C_{TDIC}$ signatures versus nitrate (Figure 12) reveals that samples with high nitrate values are depleted in $\delta^{13}C$. In fact, in the areas with dominant agricultural activities, located mainly in the center of the basin, high nitrate contents can be related to the return of irrigation water, especially where flood irrigation is still adopted with the excessive use of fertilizers.
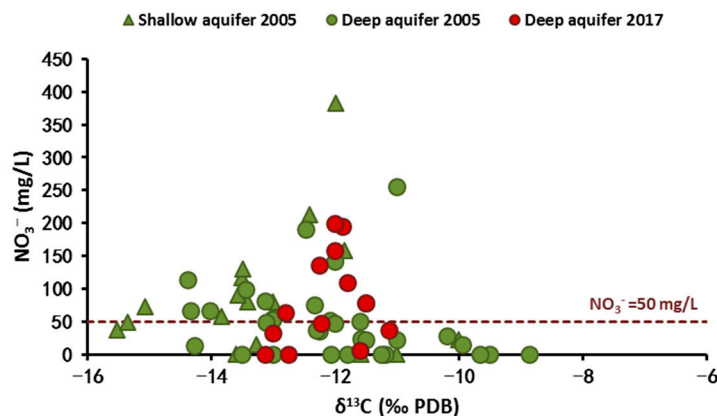

Figure 12. Plot of groundwater $\delta^{13}C_{TDIC}$ signatures versus nitrate.

Therefore, under an open aquifer system in an agricultural region, nitrate can reach the aquifer by infiltration of irrigated water and/or rainwater. The high nitrate concentrations

shown in many samples indicate the significant impact of irrigated water and wastewater discharge infiltration [25] on the aquifer recharge.

4.2.4. Carbon-14 Isotope

The radioactive carbon isotope (^{14}C) is very useful in hydrogeological studies. Characterized by long half-life, equal to 5730 ± 40 years [47], carbon-14 allows determining groundwater residence time over timescales to 30 ka [42].

The ^{14}C activities of groundwater samples, collected during the sampling campaign in 2017, range from 46.7 (Sample No. 124) to 103 ± 1 pmc (Sample No. 112) (Table S2). The most frequent values of ^{14}C fall between 60 and 80 pmc, characterizing samples located in the center and the southeastern parts of the basin (in the foothills of Abderrahman Mt.) (Figure 13a). These relatively high ^{14}C activities confirm the presence of an active groundwater recharge in these regions. This finding is in good agreement with what was previously suggested by stable isotopes and tritium contents (Figure 13b). Only two groundwater samples (Samples No. 124 and 127) show low ^{14}C activities, indicating that the recharge is relatively limited in the southern part of the basin.
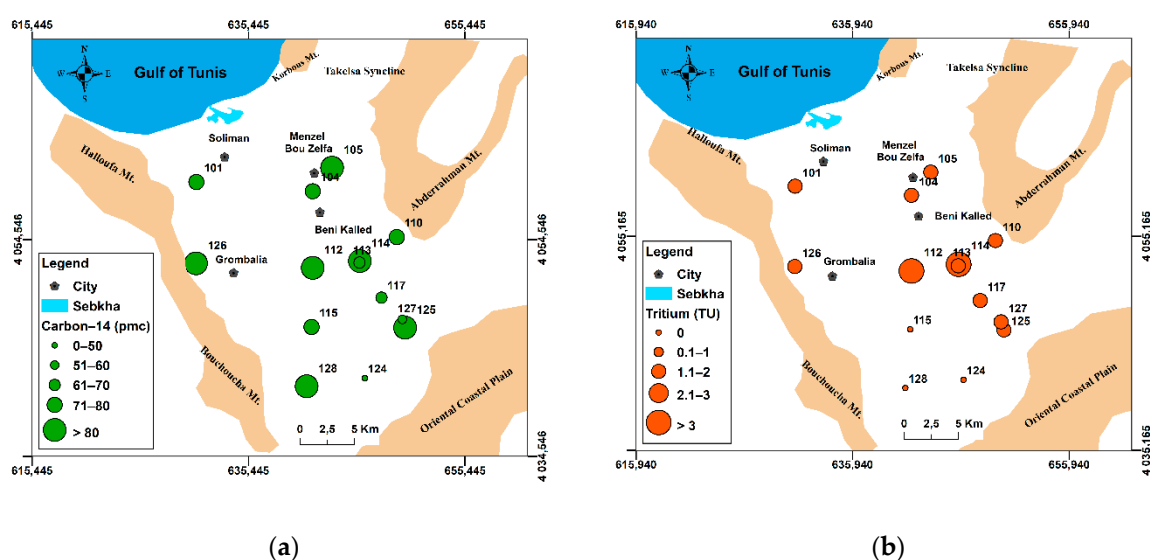

(a)   (b)

Figure 13. Distribution map of radioactive isotopes for samples collected from the deep aquifer in 2017 with: (**a**) ^{14}C activities; and (**b**) ^{3}H contents.

In the diagram of δ^{13}C versus ^{14}C activities (Figure 14a), the samples collected from deep aquifer in 2017 are compared with those collected in 2005 [17]. For the deep aquifer, 47% of the samples collected in 2005 and 43% of those collected in 2017 exceed 80 pmc for carbon-14 activities. For the shallow aquifer, most of the samples collected in 2005 (82%) have ^{14}C activities greater than 80 pmc. Overall, these activities are consistent with the recent origin of groundwater and provide insight into the existence of exchange with the soil-derived CO_2. This source of carbon agrees with the depleted δ^{13}C contents of the referred samples ranging from $-15.5\permil$ to $-10.1\permil$, from $-14.4\permil$ to $-8.9\permil$ and from $-13.1\permil$ to $-11.1\permil$ V-PDB for shallow aquifer 2005, deep aquifer 2005 and deep aquifer 2017, respectively. In this diagram, groundwater samples evolve between two end members: (1) the biogenic origin pole characterized by high activities of carbon-14 (up to 100 pmc) and depleted δ^{13}C values (close to $-16\permil$ V-PDB), indicating the significant domination of the soil-derived CO_2; and (2) the mineral pole characterized by low radiocarbon activities and relatively enriched ^{13}C values, reflecting the contribution of "dead carbon" with mineral origin.
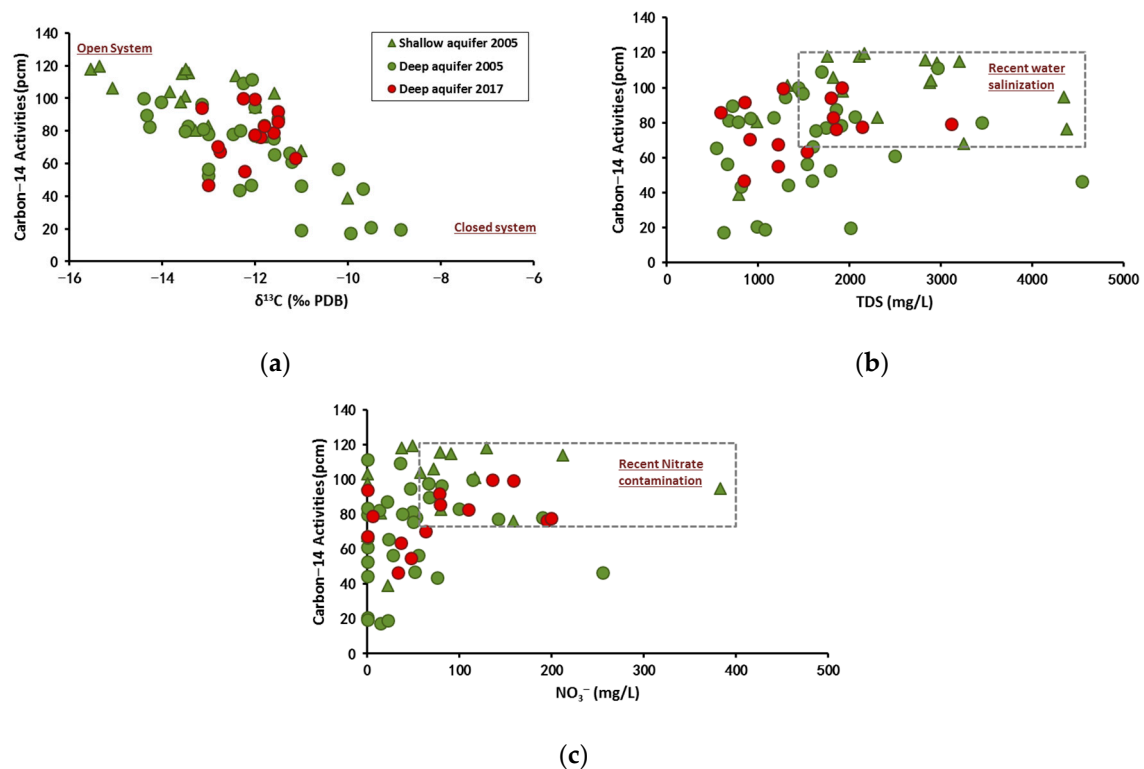
(a)

(b)

(c)

Figure 14. Variation of carbon-14 activities according to: (**a**) $\delta^{13}C$; (**b**) TDS; and (**c**) NO_3^- values.

Groundwater residence time of the collected samples is evaluated using different correction models, which are based on measured variables such as alkalinity, pH, T and ^{14}C and $\delta^{13}C$ values of dissolved inorganic carbon. These models also take into account several geochemical processes [42,48–52]. For the application of these models, the following parameters were considered:

- The ^{14}C activity of the TDIC of the samples (measured value)
- The ^{14}C activity of soil gas (A ^{14}Cg = 116 pmc)
- The ^{14}C activity of the matrix (A ^{14}Cm = 0 pmc)
- The ^{13}C content of the TDIC of the samples (measured value)
- The ^{13}C content of soil gas ($\delta^{13}Cg$ = −16‰ V-PDB)
- The ^{13}C content of the matrix ($\delta^{13}Cm$ = 0‰ V-PDB)
- Physico-chemical parameters: temperature, pH and alkalinity

The calculated ages by the different models show that most of the water samples from the deep aquifer are dated to the present day (Table 1). The application of these different models showed that: The Fontes & Garnier and IAEA models [50,51] overestimate the ages of groundwater. Evans's model is applied in the case of a carbonate reservoir considered to be infinite. It is based on the processes of dissolution and precipitation, and only precipitation is associated with isotopic fractionation. Thus, it cannot be taken in the case of the Grombalia aquifer. Eichinger's model [52] is based only on isotopic exchanges with the carbonate matrix, and, in this case, it cannot be considered for the studied basin, since, in the recharge zones, there is an exchange with the CO_2 of the soil. The models by Pearson and Tamers [48,49] show that samples are dated to the present day. The Tamers model [49], which is chemically based, gives very similar initial activities and does not take into account isotopic exchange reactions with the matrix and soil CO_2.

Table 1. Estimation of the residence time of the waters in the deep aquifer of Grombalia. Ages are expressed as Before Present (BP) years.

Sample	^{3}H	^{14}C	^{13}C	Age	Age	Age	Age	Age	Age	Age	Age
	TU	pmc	‰ V-PDB	Apparent	Brut (Ao = 100)	Tamers	Pearson	F. & G.	AIEA	Evans	Eichinger
101	0	79.03	−11.60	1890	3172	Current	514	1966	6796	380	133
104	1.31	76.46	−11.88	2156	3446	Current	984	2558	7304	865	634
105	0.29	99.38	−12	Current	1278	Current	Current	699	5195	Current	Current
110	0.77	77.67	−12	2030	3316	Current	938	2764	7208	819	583
112	1.62	103.54	−12.25	Current	940	Current	Current	724	5101	Current	Current
113	0.74	67.44	−12.72	3165	4484	Current	2587	4843	8736	2489	2240
114	1.76	94.16	−13.14	483	1724	Current	96	2916	6975	48	Current
115	0	70.43	−12.80	2816	4125	1301	2280	3231	8381	2182	1917
117	2.07	63.44	−11.13	3656	4990	29	1989	3971	8814	1887	1511
124	0	46.77	−13	6105	7510	5249	5793	6406	12340	5726	5246
125	1.2	91.84	−11.50	684	1931	Current	Current	1016	5570	Current	Current
126	0.98	82.88	−11.80	1509	2779	Current	262	1996	6632	144	Current
127	1.17	55.10	−12.23	4788	6155	2654	3933	5227	10378	3836	3595
128	1.2	85.77	−11.50	1233	2496	Current	Current	2008	5784	Current	Current

According to the diagram of δ^{13}C versus ^{14}C activities (Figure 14a), indicating an isotopic exchange occurring within the aquifer matrix, Pearson model, which is in agreement with tritium contents, appears to be the most appropriate for the Grombalia aquifer system. The corrected ages according to this model vary between the current and 5793 years PB. Even though the use of radiocarbon provides further information about the aquifer recharge and residence time, dating models are limited in the case of recent groundwater due to the fact that isotopic signature of the carbon of TDIC is mainly acquired in the unsaturated zone [53,54].

To better understand the relationship between recharge aquifer and water quality, radiocarbon activities have been plotted as a function of respective TDS and NO_3^- contents on all available data (Figure 14b,c). These diagrams indicate that the increases of salinity (TDS > 1000 mg/L) and nitrate contents ($NO_3^- > 50$ mg/L) characterize recent groundwater samples (33%). This result confirms that mineralization processes in the Grombalia aquifer system are rather related to the infiltration of recent poor-quality water, rather than to water–rock interaction, whose consequences depends on the residence time. This recent component can derive from the return of irrigation water, rich in nitrate compounds and which has undergone evaporation, and/or rainwater, which has leached the salts that have accumulated in the unsaturated zone.

The combined use of variable methods and techniques (geochemical and isotopic tracers) permitted better understanding the relationship between water quality variations and recharge process. In fact, according to chemical interpretation, the main processes controlling groundwater mineralization in Grombalia basin are especially water–rock interactions and cation exchange processes.

In addition, it is revealed that infiltration of the superficial irrigation's water enriched with nitrate fertilizers has an important role in the aquifer recharge and groundwater salinization, especially for shallow aquifer. The return flow of irrigation water was highlighted by both high nitrate concentrations and δ^{13}C values interpretation (open system). In addition, isotopic tools proved the influence of evaporation process, in semi-arid region, on groundwater salinization. This finding was highlighted by enriched water stable isotopes (δ^2H, δ^{18}O) and δ^{13}C values interpretation.

The distribution map of TDS values revealed that samples with lower salinity characterize the southeastern part of Grombalia basin, corresponding to recharge area according to tritium and carbon-14 values (high values of both tritium and carbon-14 activities). Therefore, groundwater is evolving within an open system to close system, confirming the chemical interpretation and proving the exchange with the CO_2 of the soil, especially

for the shallow aquifer. In fact, a significant component of recent water that is recharging Grombalia aquifer system is confirmed by applying correction models based on the $\delta^{13}C$ values, ^{14}C activities and ^3H contents.

The hypothesis of old origin of groundwater for some samples from the deep aquifer was based on the absence of tritium in some samples and confirmed by the low carbon-14 activities. The relationship among carbon-14 activities, TDS, nitrate values and $\delta^{13}C$ confirmed that mineralization processes in the Grombalia shallow aquifer are related to the infiltration of recent poor-quality water rather than to water–rock interaction, whose consequences depends on the residence time. In addition, the transgressive cycles that take place during the Quaternary, in coastal deposits of the Cap Bon Peninsula [55], may influence the chemical quality of groundwater. This may be explained by the potential impact of the Mediterranean Sea on mineralization and groundwater chemistry [56] (especially for the shallow aquifer) in the north part of Grombalia coastal region.

5. Conclusions

The results of the multidisciplinary investigation performed in the Grombalia aquifer permitted to better assess the hydrochemical and isotopic variation of groundwater resources.

The combined use of chemical and isotopic (δ^2H, $\delta^{18}O$, ^3H, ^{14}C and $\delta^{13}C$) tools permitted to characterize the relation between the variation of groundwater chemical composition and the aquifer recharge.

The results indicate that salinity exceeds 1000 mg/L in the most of samples, especially for the shallow aquifer, except in recharge area, thus making the water not recommended for drinking water.

According to major ionic ratios and HFE-Diagram, the groundwater mineralization of Grombalia basin is governed by several processes: the evaporates dissolution such as halite and gypsum, evaporation, return flow of irrigation water and inverse cation exchange process triggered by a possible marine intrusion. In fact, groundwater mineralization is also conditioned by the residence time of the water within the aquifer. The application of isotopic tools (^{14}C and $\delta^{13}C$) revealed that groundwater is evolving within an open system to close system.

Aquifer recharge is mainly associated to the direct infiltration of recent rainwater, the return flow of irrigation water and in small part by artificial recharge. In particular, for the shallow aquifer, the impact of irrigated water infiltration on the aquifer recharge is very significant. For the deep aquifer, it reveals the existence of two recharge periods: pre-nuclear and post-nuclear tests in 1952, according to tritium concentrations. The residence time of groundwater in deep aquifer, estimated by carbon-14 activities and corrected by applying correction models based on the $\delta^{13}C$ values, varies between the current and 5793 years BP according to the Pearson model.

Contrary to previous studies focused on Grombalia basin, explaining the increase of salinity by dominant water–rock interaction processes, the effect of which depends on residence time, this study showed that the increase in salinity also depends on the infiltration of recent water with poor quality. This water has an origin whether from the infiltration of irrigation water or from rainwater which has leached the salts that accumulate in the unsaturated zone due to the used irrigation method, the impact of wastewater discharge and the aridity of the climate.

These findings may therefore be useful to support new regional policies to further constraint aquifer salinization and pollution. To this end, future steps involve the presentation of the results to local water authorities and the civil society to discuss possible joint and shared actions for the long-term groundwater resources in the region. Local stakeholders, involved since the early stages of the project [25,57], will be key for the successful translation of scientific findings into concrete actions, and the successful socio-hydrogeological investigation in the Grombalia region can represent a valuable example to be replicated in the Mediterranean Basin.

References

1. Ouhamdouch, S.; Bahir, M.; Ouazar, D.; Carreira, P.M.; Zouari, K. Evaluation of climate change impact on groundwater from semi-arid environment (Essaouira Basin, Morocco) using integrated approaches. *Environ. Earth Sci.* **2019**, *78*, 449. [CrossRef]
2. Rakib, M.A.; Sasaki, J.; Matsuda, H.; Quraishi, S.B.; Mahmud, M.J.; Bodrud, D.M.; Bhuiyan, M.A. Groundwater salinization and associated co-contamination risk increase severe drinking water vulnerabilities in the southwestern coast of Bangladesh. *Chemosphere J.* **2020**, *246*, 125646. [CrossRef] [PubMed]
3. Bani, A.; Daghari, I.; Hatira, A.; Chaabane, A.; Daghari, H. Sustainable management of a cropping system under salt stress conditions (Korba, Cap-Bon, Tunisia). *Environ. Sci. Pollut. Res.* **2020**, 1–8. [CrossRef]
4. Krishan, G. Groundwater Salinity. *Curr. World Environ.* **2019**, *14*, 186. [CrossRef]
5. Bahir, M.; Ouazar, D.; Ouhamdouch, S.; Zouari, K. Assessment of groundwater mineralization of alluvial coastal aquifer of essaouira basin (Morocco) using the hydrochemical facies evolution diagram (HFE-Diagram). *Groundw. Sustain. Dev.* **2020**, *11*, 100487. [CrossRef]
6. Gana, A.; Fouillen, B. Concurrences et Conflits Pour L'usage de L'eau en Tunisie: Étude de cas Dans la Région du Cap Bon, Le Carnet de l'IRMC, 21 February 2014. Available online: http://irmc.hypotheses.org/1412 (accessed on 21 February 2014).
7. Gaaloul, N.; Candela, L.; Chebil, A.; Soussi, A.; Tamoh, K. Groundwater flow simulation at the Grombalia phreatic aquifer (Cap Bon, Northeastern Tunisia). *Desalin. Water Treat.* **2014**, *52*, 1997–2008. [CrossRef]
8. Trabelsi, R.; Zouari, K.; Kammoun, S.; Trigui, M.R. Recharge and paleo-recharge of groundwater in different basins in Tunisia. *Quat. Int.* **2020**, *547*, 152–165. [CrossRef]
9. Zaidi, F.K.; Nazzal, Y.; Jafri, M.K.; Naeem, M.; Ahmed, I. Reverse ion exchange as a major process controlling the groundwater chemistry in an arid environment: A case study from northwestern Saudi Arabia. *Environ. Monit. Assess.* **2015**, *187*, 607. [CrossRef]
10. Kammoun, S.; Trabelsi, R.; Re, V.; Zouari, K.; Henchiri, J. Groundwater Quality Assessment in Semi-Arid Regions Using Integrated Approaches: The Case of Grombalia Aquifer (NE Tunisia). *Environ. Monit. Assess.* **2018**, *190*, 87. [CrossRef]
11. Kammoun, S.; Re, V.; Trabelsi, R.; Zouari, K.; Daniele, S. Assessing Seasonal Variations and Aquifer Vulnerability in Coastal Aquifers of Semi-Arid Regions Using a Multi-Tracer Isotopic Approach: The Case of Grombalia (Tunisia). *Hydrogeol. J.* **2018**, *26*, 2575–2594. [CrossRef]
12. Gaaloul, N. Gestion intégrée des ressources en eaux souterraines: Cas de la plaine du Cap Bon. *La Houille Blanche* **2008**, *5*, 38–44. [CrossRef]
13. Charfi, S.; Zouari, K.; Feki, S.; Mami, E. Study of variation in groundwater quality in a coastal aquifer in north-eastern Tunisia using multivariate factor analysis. *Quat. Int.* **2013**, *302*, 199–209. [CrossRef]

14. Lachaal, F.; Chekirbane, A.; Chargui, S.; Sellami, H.; Tsujimura, M.; Hezzi, H.; Mlayah, A. Water resources management strategies and its implications on hydrodynamic and hydrochemical changes of costal groundwater: Case of Grombalia shallow aquifer, NE Tunisia. *J. Afr. Earth Sci.* **2016**, *124*, 171–188. [CrossRef]

15. Lachaal, F.; Chargui, S.; Messaoud, R.B.; Chekirbane, A.; Tsujimura, M.; Mlayah, A.; Leduc, C. Impacts of global changes on groundwater resources in north-east Tunisia: The case of the Grombalia phreatic aquifer. In *Groundwater and Global Change in the Western Mediterranean Area*; Springer: Cham, Switzerland, 2018; pp. 179–188.

16. Moussa, A.B.; Zouari, K. *Hydrochemical Investigation of Groundwater Contamination in the Grombalia Shallow Aquifer, Cap Bon Peninsula, Tunisia: Impact of Irrigation with Industrial Waste Water*; Tech Open Access: Rijeka, Croatia, 2011; pp. 239–252.

17. Charfi, S.; Trabelsi, R.; Zouari, K.; Chkir, N.; Charfi, H.; Rekaia, M. Isotopic and hydrochemical investigation of the Grombalia deep aquifer system, northeastern Tunisia. *Carbonates Evaporites* **2013**, *28*, 281–295. [CrossRef]

18. CRDA. *Annuaire de L'exploitation des Nappes Souterraines de L'année 2014 [Yearbook of Groundwater Exploitation of the Year 2014]*; Technical Report; CRDA: Tunis, Tunisia, 2014.

19. Simler, R.; Diagrammes. Laboratoire D'hydrogeologie D'avignon, Université D'avignon, Logiciel D'hydrochimie Multilangage en Distribution Libre. 2004. Available online: http://www.lha.univ-avignon.fr (accessed on 20 October 2020).

20. Penna, D.; Stenni, B.; Wrede, S.; Bogaard, T.A.; Gobbi, A.; Borga, M.; Fischer, B.M.C.; Bonazza, M.; Charova, Z. On the reproducibility and repeatability of laser absorption spectroscopy measurements for [delta] ^{2}H and [delta] ^{18}O isotopic analysis. *Hydrol. Earth Syst. Sci.* **2010**, *14*, 1551. [CrossRef]

21. Taylor, C.B. *IAEA Isotope Hydrology Laboratory Technical Procedure*; Note No.19; International Atomic Energy Agency: Vienna, Austria, 1976; pp. 1–30.

22. Fontes, J.C. Un ensemble destiné à la mesure de l'activité du radiocarbone naturel par scintillation liquide. *Rev. Géog. Phys. Géol. Dyn.* **1971**, *13*, 67–86.

23. WHO, World Health Organisation. *Guidelines for Drinking-Water Quality*, 4th ed.; Incorporating First Addendum: Geneva, Switzerland, 2017; ISBN 978-92-4-254995-9.

24. Tlili, Z.B.; Hamzaoui, A.F.; Gueddari, M.; Bouhlila, R. Geochemistry and quality assessment of groundwater using graphical and multivariate statistical methods. A case study: Grombalia phreatic aquifer (Northeastern Tunisia). *Arab. J. Geosci.* **2013**, *6*, 3545–3561. [CrossRef]

25. Re, V.; Sacchi, E.; Kammoun, S.; Tringali, C.; Trabelsi, R.; Zouari, K.; Daniele, S. Integrated socio-hydrogeological approach to tackle nitrate contamination in groundwater resources. The case of Grombalia Basin (Tunisia). *Sci. Total Environ.* **2017**, *593*, 664–676. [CrossRef]

26. Fisher, R.S.; Mullican, W.F. Hydrochemical evolution of sodium-sulphate and sodium-chloride groundwater beneath the Northern Chihuahuan desert, Trans-Pecos, Texas, USA. *Hydrogeol. J.* **1997**, *5*, 4–16. [CrossRef]

27. Rajmohan, N.; Elango, L. Identification and evolution of hydrogeochemical processes in the groundwater environment in an area of the Palar and Cheyyar River Basins, Southern India. *Environ. Geol.* **2004**, *46*, 47–61. [CrossRef]

28. Garcia, G.M.; Hidalgo, M.D.V.; Blesa, M.A. Geochemistry of groundwater in the alluvial plain of Tucuman province, Argentina. *Hydrogeol. J.* **2001**, *9*, 597–610. [CrossRef]

29. Lean, W.; Jankowski, J.; Lavitt, N. Groundwater quality and sustainability in an alluvial aquifer, Australia. In *Groundwater, Past Achievements and Future Challenges*; A. A. Balkema Publishers: Rotterdam, The Netherlands, 2000; pp. 567–573.

30. Giménez, F.E. Dynamic of sea water interface using hydrochemical facies evolution diagram. *Groundwater* **2010**, *48*, 212–216. [CrossRef] [PubMed]

31. Han, D.; Song, X.; Currell, M.J. Identification of anthropogenic and natural inputs of SO_4 into a karstic coastal groundwater system in northeast China, Evidence from major ions, δ^{13} CDIC and δ^{34} S$_{SO_4}$. *Hydrol. Earth Syst. Sci.* **2016**, *20*, 1983–1999. [CrossRef]

32. Van, L.T.T.; Lertsirivorakul, R.; Bui, T.V.; Schulmeister, M.K. An application of HFE-D for evaluating seawater intrusion in coastal aquifers of Southern Vietnam. *Groundwater* **2020**. [CrossRef]

33. Kumar, P.S. Deciphering the groundwater–saline water interaction in a complex coastal aquifer in South India using statistical and hydrochemical mixing models. *Model. Earth Syst. Environ.* **2016**, *2*, 1–11. [CrossRef]

34. Giménez, F.E. Use of the Hydrochemical Facies Diagram (HFE-D) for the evaluation of salinization by seawater intrusion in the coastal Oropesa Plain: Comparative analysis with the coastal Vinaroz Plain, Spain. *HydroResearch* **2019**, *2*, 76–84. [CrossRef]

35. Appelo, C.A.J.; Willemsen, A. Geochemical calculations and observations on salt water intrusions, I. A combined geochemical/mixing cell model. *J. Hydrol.* **1987**, *94*, 313–330. [CrossRef]

36. Fontes, J.C. *Isotopes du Milieu et Cycle des Eaux Naturelles: Quelques Aspects*; Thèse de Doctorat en Sciences, Université de Paris: Paris, France, 1976.

37. Rozanski, K.; Araguás, A.L.; Gonfiantini, R. Isotopic patterns in modern global precipitation. *Geophys. Monogr.* **1993**, *78*, 1–36.

38. Zouari, K.; Aranyossy, J.F.; Mamou, A.; Fontes, J.C. *Etude isotopique et géochimique des mouvements et de l'évolution des solutions de la zone aérée des sols sous climat semi-aride (Sud tunisien)*; Stable and Radioactive Isotopes in the Study of the Unsaturated Soil Zone; IAEA-TECDOC-357: Vienna, Austria, 1985; pp. 121–144.

39. GNIP. Global network of isotopes in precipitation. In *Atlas of Isotopes Hydrology*; IAEA: Vienna, Austria, 2007; pp. 89–93.

40. Dulinski, M.; Rozanski, K.; Kania, J.; Karlikowska, J.; Korczynski, J.M.; Witczak, S.; Mochalski, P.; Opoka, M.; Sliwka, I.; Zuber, A. *Groundwater Dating with Sulfur Hexafluoride: Methodology and Field Comparison with Tritium and Hydrodynamic Methods*; International Atomic Energy Agency: Vienna, Austria, 2003.

41. Lucas, L.L.; Unterweger, M.P. Comprehensive Review and critical Evaluation of the Half-Life of Tritium. *J. Res. Natl. Inst. Stand. Technol.* **2000**, *105*, 541–549. [CrossRef]

42. Clark, I.; Fritz, P. *Environmental Isotopes in Hydrogeology*; CRC Press: Boca Raton, FL, USA, 1997; Volume I, pp. 104–328.

43. Driscoll, F.G. *Groundwater and Wells*; Jonhson Division Publishers: Saint-Paul, MN, USA, 1986; p. 1089.

44. Weijden, C.H.; Pacheco, F.A.L. Hydrochemistry, weathering and weathering rates on Madeira Island. *J. Hydrol.* **2003**, *283*, 122–145. [CrossRef]

45. Adams, S.; Tredoux, G.; Harris, C.; Titus, R.; Pietersen, K. Hydrochemical characteristics of aquifers near Sutherland in the Western Karoo, South Africa. *J. Hydrol.* **2001**, *241*, 91–103. [CrossRef]

46. Awad, S. Analysing groundwater using the ^{13}C isotope. *Phys. Procedia* **2014**, *55*, 35–40. [CrossRef]

47. Mook, W.G.; Vries, J.J. Environmental Isotopes in Hydrogeological Cycle-Principles and Applications. In *Technical Documents in Hydrology*; International Atomic Energy Agency (UNESCO/IAEA): Paris, France, 2000; Volumes 1–6.

48. Pearson, F.J.; Hanshaw, B.B. Sources of dissolved carbonate species in groundwater and their effects on carbon-14 dating. *Isot. Hydrol.* **1970**, *1970*, 271–285.

49. Tamers, M.A. Validity of radiocarbon dates on groundwater. *Geophys. Surv.* **1975**, *2*, 217–239. [CrossRef]

50. Fontes, J.C.; Garnier, J.M. Determination of the initial ^{14}C activity of the total dissolved carbon. A review of the existing models and a new approach. *Water Resour. Res.* **1979**, *12*, 399–413. [CrossRef]

51. Salem, O.; Visser, J.H.; Dray, M.; Gonfiantini, R. Groundwater flow patterns in the western Libyan Arab Jamahiriya. In *Arid Zone Hydrogeology*; Investigations with Isotope Techniques; IAEA: Vienna, Austria, 1980; pp. 165–179.

52. Eichinger, E. A contribution to the interpretation of ^{14}C groundwater ages considering the example of partially confined sandstone aquifer. *Radiocarbon* **1983**, *25*, 347–356. [CrossRef]

53. Gillon, M.; Barbecot, F.; Gibert, E.; Alvarado, J.C.; Marlin, C.; Massault, M. Open to closed system transition traced through the TDIC isotopic signature at the aquifer recharge stage, implications for groundwater ^{14}C dating. *Geochim. Cosmochim. Acta* **2009**, *73*, 6488–6501. [CrossRef]

54. Fang, S.C. Study on ^{14}C dating analysis of deep groundwater resources on islands. *J. Environ. Radioact.* **2019**, *208*, 105994. [CrossRef]

55. Chakroun, A.; Zaghbib, T.D.; Miskovsky, J.C.; Davaud, E. Two Tyrrhenian transgressive cycles in coastal deposits of the Cap Bon Peninsula, Tunisia. *Quaternaire. Rev. Assoc. Française Étude Quat.* **2009**, *20*, 215–226. [CrossRef]

56. Re, V.; Zuppi, G.M. Influence of precipitation and deep saline groundwater on the hydrological systems of Mediterranean coastal plains: A general overview. *Hydrol. Sci. J.* **2011**, *56*, 966–980. [CrossRef]

57. Tringali, C.; Re, V.; Siciliano, G.; Chkir, N.; Tuci, C.; Zouari, K. Insights and participatory actions driven by a socio-hydrogeological approach for groundwater management: The Grombalia Basin case study (Tunisia). *Hydrogeol. J.* **2017**, *25*, 1241–1255. [CrossRef]